The Astrophysical Journal, 870:124 (9pp), 2019 January 10 https://doi.org/10.3847/1538-4357/aaf3a4

Confirming the Presence of Second-population Stars and the Iron Discrepancy along the AGB of the Globular Cluster NGC 6752*

A. Mucciarelli[1,2], E. Lapenna[1,2], C. Lardo[3], P. Bonifacio[4], F. R. Ferraro[1,2], and B. Lanzoni[1,2]
[1] Dipartimento di Fisica e Astronomia, Università degli Studi di Bologna, Via Gobetti 93/2, I-40129 Bologna, Italy; alessio.mucciarelli2@unibo.it
[2] INAF—Osservatorio di Astrofisica e Scienza dello Spazio di Bologna, Via Gobetti 93/3, I-40129 Bologna, Italy
[3] Laboratoire d'astrophysique, Ecole Polytechnique Fèdèrale de Lausanne (EPFL), Observatoire de Sauverny, 1290, Versoix, Switzerland
[4] GEPI, Observatoire de Paris, Université PSL, CNRS, Place Jules Janssen, F-92195 Meudon, France
Received 2018 October 12; revised 2018 November 22; accepted 2018 November 23; published 2019 January 16

Abstract

Asymptotic giant branch (AGB) stars in the globular cluster NGC 6752 have been found to exhibit some chemical peculiarities with respect to the red giant branch (RGB) stars. A discrepancy between [Fe I/H] and [Fe II/H] (not observed in RGB stars) has been detected adopting spectroscopic temperatures. Moreover, a possible lack of second-population stars along the AGB was claimed. The use of photometric temperatures based on $(V-K)$ colors was proposed to erase this iron discrepancy. Also, ad hoc scenarios have been proposed to explain the absence of second-population AGB stars. Here we analyzed a sample of 19 AGB and 14 RGB stars of NGC 6752 observed with the spectrograph's UVES. The two temperature scales agree very well for the RGB stars while for the AGB stars there is a systematic offset of ∼100 K. We found that even if the photometric temperatures alleviate the iron discrepancy with respect to the spectroscopic ones, a systematic difference between [Fe I/H] and [Fe II/H] is still found among the AGB stars. An unexpected result is that the photometric temperatures do not satisfy the excitation equilibrium in the AGB stars. This suggests that standard 1D-LTE model atmospheres are unable to properly describe the thermal structure of AGB stars, at variance with the RGB stars. The use of photometric temperatures confirms the previous detection of second-population AGB stars in this cluster, with the presence of clear correlations/anticorrelations among the light element abundances. This firmly demonstrates that both first- and second-population stars evolve along the AGB of NGC 6752.

Key words: globular clusters: individual (NGC 6752) – stars: abundances – stars: AGB and post-AGB – techniques: spectroscopic

1. Introduction

Two main results obtained in recent years have revived the interest in the chemical composition of asymptotic giant branch (AGB) stars in globular clusters (GCs). First, was the discovery that iron abundances derived from neutral and single ionized Fe lines systematically differ in AGB stars (Ivans et al. 2001; Lapenna et al. 2014, 2015; Mucciarelli et al. 2015a, 2015b). In particular, Fe I lines provide lower abundances (by 0.15–0.25 dex) with respect to Fe II lines, only the latter providing abundances consistent with those measured in red giant branch (RGB) stars of the same cluster. This iron discrepancy has not been observed among the RGB stars, where the two sets of Fe lines provide consistent abundances. A qualitative explanation of this discrepancy, originally proposed by Ivans et al. (2001), is that nonlocal thermodynamical equilibrium (NLTE) effects, which significantly impact neutral lines but only marginally affect single ionized lines, are present in the atmospheres of AGB stars. However, this interpretation is not fully satisfactory because the NLTE corrections predicted by current theoretical models are similar for AGB and RGB stars (see, e.g., Bergemann et al. 2012; Lind et al. 2012).

Second, it has been speculated that some cluster stars characterized by a strong enhancement in N and Na and a depletion in C and O fail to ascend the AGB phase. These stars (usually called second-population stars, hereafter 2P stars) should have formed from the gas ejected by the first stars formed in the cluster (the so-called first population stars, hereafter 1P stars) and characterized by light element abundances that well resemble those measured in field stars of similar metallicity. It is now well established that all old and massive clusters host a mixture of 1P and 2P stars, and the fraction of 2P stars strongly correlates with present-day GC mass (see, e.g., Gratton et al. 2012; Bastian & Lardo 2018). However, it has also been observed that the fraction of 2P stars along the AGB is generally smaller than that of the RGB phase in a given cluster. Early evidence of this difference is based on the analysis of CN molecular bands in low-resolution spectra (Norris et al. 1981; Smith & Norris 1993), but recent studies based on high-resolution spectra confirm this finding (see, e.g., Campbell et al. 2013; Lapenna et al. 2015, 2016; Wang et al. 2017). This can be explained by the fact that 2P stars should also be He rich and have a lower mass than 1P stars. According to standard stellar evolution, stars with masses below 0.55 $M_{\odot}$ are expected to skip the AGB phase after the central He-burning phase (the so-called AGB-manqué stars, see, e.g., Greggio & Renzini 1990).

The existence and the extent of both the iron discrepancy and the dearth of 2P stars along the AGB are still highly debated, with the nearby GC NGC 6752 representing one of the most intriguing cases. Campbell et al. (2013, hereafter C13) derived the Na abundance of 20 AGB cluster stars using GIRAFFE-FLAMES@VLT spectra and concluded that they all belong to 1P. Since this is not expected from standard stellar evolution (Cassisi et al. 2014), a very strong mass loss in 2P stars during the horizontal branch phase has been invoked by C13 to account for the observed lack of 2P AGB stars. However, this

* Based on observations collected at ESO-VLT under programs 073.D-0211 and 095.D-0320.

assumption is not supported by current models of stellar wind in horizontal branch stars (Vink & Cassisi 2002).

Lapenna et al. (2016, hereafter L16) analyzed the same stars presented in C13 reobserved at higher spectral resolution with the spectrograph UVES@VLT. They found that (1) the iron abundances measured from Fe I lines are lower (by about 0.2 dex) than those derived from Fe II features, confirming the occurrence of the iron discrepancy also in the AGB population of NGC 6752 (note that C13 did not directly measure iron abundances from their spectra, but they assumed a constant Fe abundance from the literature); and (2) 2P stars are present also along the AGB (in contrast with the conclusions reached by C13), and the AGB stars show clear evidence of C–N, Na–O anticorrelations and N–Na, Al–Na correlations. The analysis by L16 demonstrates that the AGB population of NGC 6752 is composed of a mixture of 1P and 2P stars, lacking only the most extreme population (characterized by the highest Na and the lowest O abundances) which is observed among the RGB stars of the cluster. This result agrees with the expectations from standard stellar evolution (see, e.g., Cassisi et al. 2014) and it has been recently confirmed by Gruyters et al. (2017) using Strömgren photometry.

Campbell et al. (2017, hereafter C17) then questioned the result obtained by L16. They concluded that the iron discrepancy found by L16 is due to the use of spectroscopic effective temperatures ($T_{\rm eff}$), while the adoption of $T_{\rm eff}$ based on the classical infrared flux method (IRFM, originally proposed by Blackwell & Shallis 1977) and the $(V-K)_0$ broadband color, reconciles the abundances obtained from Fe I and Fe II lines. Moreover, C17 argued that the light element correlations/anticorrelations derived by L16 should be revised in light of the proposed photometric $T_{\rm eff}$ scale.

Another still debated case is M4, for which the chemical analyses by MacLean et al. (2016, 2018) suggest a clear lack of 1P stars along the AGB (at variance with the RGB), while opposite results have been obtained by Lardo et al. (2017), who found a comparable broadening of AGB and RGB sequences using the $C_{\rm UBI}$ index sensitive to the light element abundances, and by Marino et al. (2017), who detected the Na–O anticorrelation among the AGB stars using UVES-FLAMES spectra.

In this paper we present a reanalysis of the spectra of AGB stars in NGC 6752 originally discussed in L16 using the $T_{\rm eff}$ scales indicated by L16 and C17 to conclusively assess their impact on the measure of Fe I, Fe II, C, N, O, Na, and Al chemical abundances.

2. Observational Data

We analyzed two different spectroscopic data sets of stars in NGC 6752:

AGB sample. We used the high-resolution spectra collected with the UVES spectrograph (Dekker et al. 2000) at the ESO-VLT (under the program 095.D-0320, PI:Mucciarelli) for 20 AGB cluster stars, already analyzed in L16. The targets are the same as those previously discussed in C13 and revised in C17. Because C17 derived new photometric $T_{\rm eff}$ for only 19 out 20 AGB stars of the original sample of C13, in the following we restrict the analysis to those stars only. The observations have been obtained with the Dichroic1 mode employing the gratings 390 Blue Arm CD#2 and 580 Red Arm CD#3, and adopting the 1 arcsec slit that provides a spectral resolution of 40,000. More details on the observations and data reduction can be found in L16.

RGB sample. As a reference sample, we analyzed archival high-resolution spectra for 14 RGB cluster stars secured with UVES-FLAMES@VLT (Pasquini et al. 2000) under program 073.D-0211 (PI:Carretta). The observations have been performed adopting the setup 580 Red Arm CD#3. We refer the reader to Carretta et al. (2009) for more details on the observations.

3. Chemical Analysis

The chemical abundances of Fe, Na, and Al have been determined by using the code GALA (Mucciarelli et al. 2013) through the measurement of the equivalent widths of unblended lines. The equivalent widths have been measured using the code DAOSPEC (Stetson & Pancino 2008) managed through the wrapper 4DAO (Mucciarelli 2013). The abundances of C, N, and O have been obtained through our own code SALVADOR that performs a *chi-square* minimization between observed and synthetic spectra, the latter is calculated with the code SYNTHE (Sbordone et al. 2004; Kurucz 2005). We refer to L16 for details about the analysis procedure and the selection of the used transitions.

We derived chemical abundances using two sets of atmospheric parameters:

1. The first set of atmospheric parameters is that obtained by using the *hybrid method* described in Mucciarelli et al. (2015a) and already adopted by L16 for the AGB sample. In this approach $T_{\rm eff}$ are derived spectroscopically through the excitation equilibrium, by flattening the slope between the Fe I line abundances, and the excitation potential, χ. Surface gravities (log g) have been derived through the Stefan–Boltzmann relation, adopting the spectroscopic $T_{\rm eff}$, a distance modulus $(m-M)_V =$ 13.13 mag (Harris 1996), a color excess $E(B-V) =$ 0.04 mag (Ferraro et al. 1999), and stellar masses of 0.80 and 0.61 $M_\odot$ for RGB and AGB targets, respectively. Microturbulent velocities (v_t) have been obtained by requiring no trend between iron abundances and the reduced equivalent widths. This approach is suitable for high-quality, large spectral coverage spectra for which robust spectroscopic $T_{\rm eff}$ can be derived, avoiding the risk of incorrect spectroscopic log g in case of NLTE or other systematic discrepancies between Fe I and Fe II lines (that could affect the AGB stars).
2. The second set of parameters adopted here has been obtained with the method used by C17 who photometrically derived $T_{\rm eff}$ and log g. In particular, C17 derived $T_{\rm eff}$ using the IRFM as implemented by Casagrande et al. (2010) and adopting the broadband $(V-K)_0$ color. We reanalyzed the AGB target stars adopting the values of $T_{\rm eff}$ and log g calculated by C17, while v_t have been derived spectroscopically to take advantage of the large number of Fe lines available in the UVES spectra (at variance with C17, who derived this parameter adopting the log g–v_t relation by Gratton et al. 1996).

For the RGB stars, we derived $T_{\rm eff}$ using the $(V-K)_0$–$T_{\rm eff}$ relation provided by Casagrande et al. (2010), while log g have been obtained from the Stefan–Boltzmann relation. As was done by C17, we adopted the optical photometry by Momany et al. (2002) and the near-infrared photometry from the 2MASS database (Skrutskie et al. 2006).

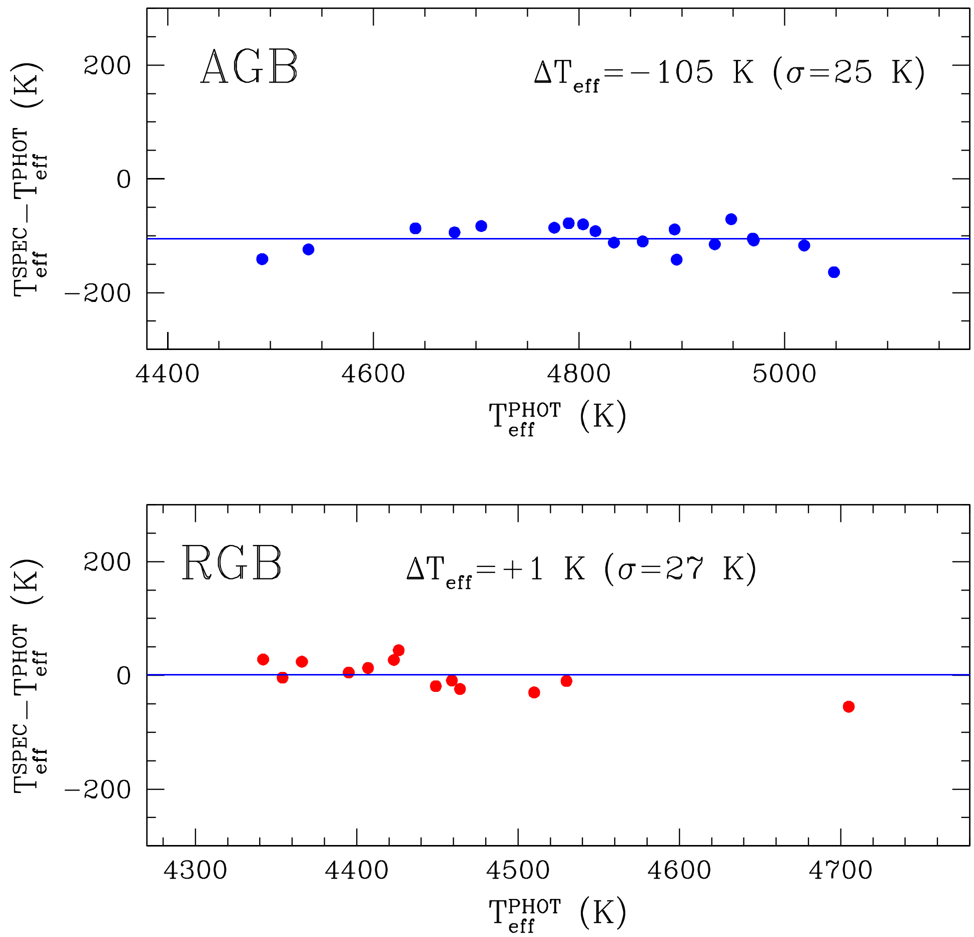

Figure 1. Difference between spectroscopic and photometric $T_{\rm eff}$ as a function of the photometric $T_{\rm eff}$ for AGB and RGB samples (upper and lower panel, respectively). The blue solid lines mark the average difference values, which are also labeled in each panel.

Table 1
Average [Fe I/H] and [Fe II/H] Abundance Ratios for the AGB and RGB Samples, Adopting Photometric and Spectroscopic $T_{\rm eff}$

$T_{\rm eff}$	$[\mathrm{Fe\,I/H}]_{\rm RGB}$	$[\mathrm{Fe\,II/H}]_{\rm RGB}$	$[\mathrm{Fe\,I/H}]_{\rm AGB}$	$[\mathrm{Fe\,II/H}]_{\rm AGB}$
PHOT	-1.60 ± 0.01 ($\sigma = 0.04$)	-1.58 ± 0.01 ($\sigma = 0.02$)	-1.69 ± 0.01 ($\sigma = 0.04$)	-1.57 ± 0.01 ($\sigma = 0.02$)
SPEC	-1.60 ± 0.01 ($\sigma = 0.03$)	-1.58 ± 0.01 ($\sigma = 0.03$)	-1.81 ± 0.01 ($\sigma = 0.05$)	-1.58 ± 0.01 ($\sigma = 0.02$)

We compare the two sets of adopted $T_{\rm eff}$ for AGB and RGB stars, separately. Figure 1 shows the difference between spectroscopic and photometric $T_{\rm eff}$ as a function of the photometric $T_{\rm eff}$ for the two samples. For the AGB stars the average difference is $\Delta T_{\rm eff} = -105$ K ($\sigma = 25$ K), indicating a systematic offset between the two scales, while for the RGB stars the two scales agree very well, with an average difference of only $+1$ K ($\sigma = 27$ K).

4. Results

In this section we quantitatively investigate the dependence of the derived abundances on the adopted atmospheric parameters discussed in Section 3.

1. *Iron discrepancy*. Table 1 reports the average Fe abundances from neutral and single ionized lines for AGB and RGB stars obtained by using the two $T_{\rm eff}$ scales. Figure 2 shows the Fe I and Fe II metallicity distributions for the two stellar samples, obtained by adopting the photometric (left panels) and the spectroscopic (right panels) $T_{\rm eff}$ scales. The metallicity distributions are shown as generalized histograms, a representation that removes the effects due to the choice of the starting point and of the bin size by taking the uncertainties in each individual [Fe/H] value into account (Laird et al. 1988).

   For the RGB stars photometric and spectroscopic $T_{\rm eff}$ agree very well (see Figure 1), leading to very similar iron abundances both from Fe I and Fe II lines. In the case of the AGB stars, a significant difference remains between [Fe I/H] and [Fe II/H] regardless of the adopted $T_{\rm eff}$. In particular, the difference between [Fe I/H] and [Fe II/H] is of -0.23 dex if spectroscopic $T_{\rm eff}$ are assumed, and -0.12 dex with the photometric $T_{\rm eff}$. The higher values of $T_{\rm eff}$ derived from C17 lead to an increase of [Fe I/H] (a change of ± 100 K leads to a variation of ± 0.12 dex in [Fe I/H]). We also stress that Fe II lines in AGB stars provide the same abundance found for RGB stars from both neutral and single ionized lines, regardless of the adopted $T_{\rm eff}$, confirming that Fe II lines are the most reliable indicator of metallicity for these stars.

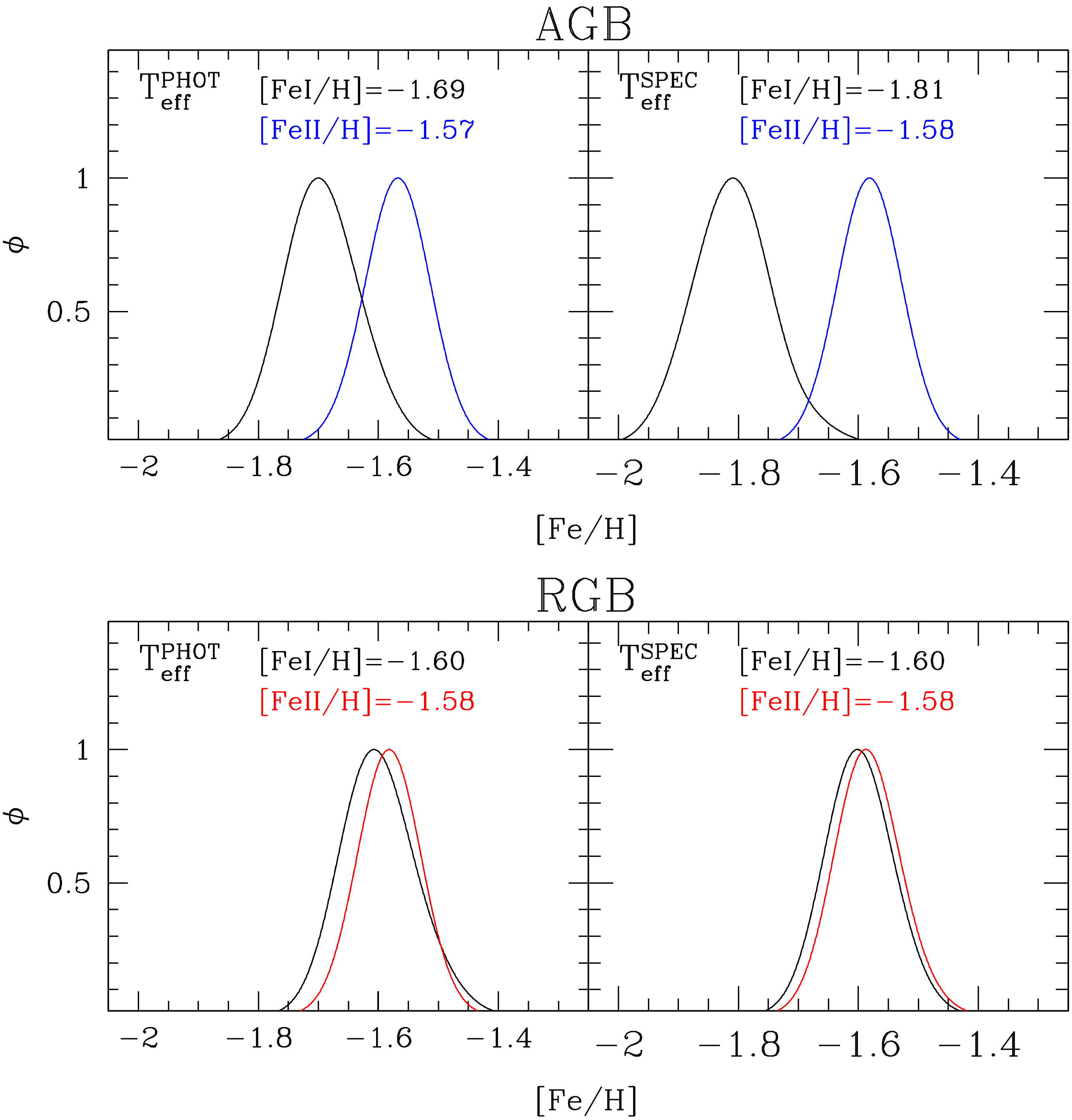

Figure 2. [Fe/H] distributions for the AGB and RGB samples (upper and lower panels, respectively) as derived from Fe I (black histograms) and Fe II lines (blue and red histograms). The left panels show the [Fe/H] distributions obtained with the photometric T_{eff} scale used by C17, while the right panels display those obtained with the spectroscopic T_{eff}.

As a further check, we also reanalyzed the archival GIRAFFE spectra used by C13 and C17, adopting the atmospheric parameters derived by C17 and a suitable line list, including Fe lines predicted to be unblended according to the cluster metallicity, the stellar parameters, and the spectral resolution of GIRAFFE. For AGB stars we derived [Fe I/H] = −1.68 ± 0.01 dex (σ = 0.05 dex) and [Fe II/H] = −1.56 ± 0.01 dex (σ = 0.03 dex). For the RGB stars observed by C13 and C17 (a different sample with respect to the reference one analyzed here and described in Section 2) we derived [Fe I/H] = −1.58 ± 0.01 dex (σ = 0.04 dex) and [Fe II/H] = −1.55 ± 0.01 dex (σ = 0.05 dex), in perfect agreement with the results obtained from the two UVES samples.

2. *Light element abundances*. Figure 3 shows the C–N and O–Na anticorrelations and the N–Na and Na–Al correlations obtained for the AGB stars of NGC 6752 using the spectroscopic T_{eff} scale by L16 (blue empty circles) and the photometric one of C17 (blue filled circles). The two sets of abundance ratios (normalized to hydrogen) exhibit the same patterns. The difference of about 100 K between

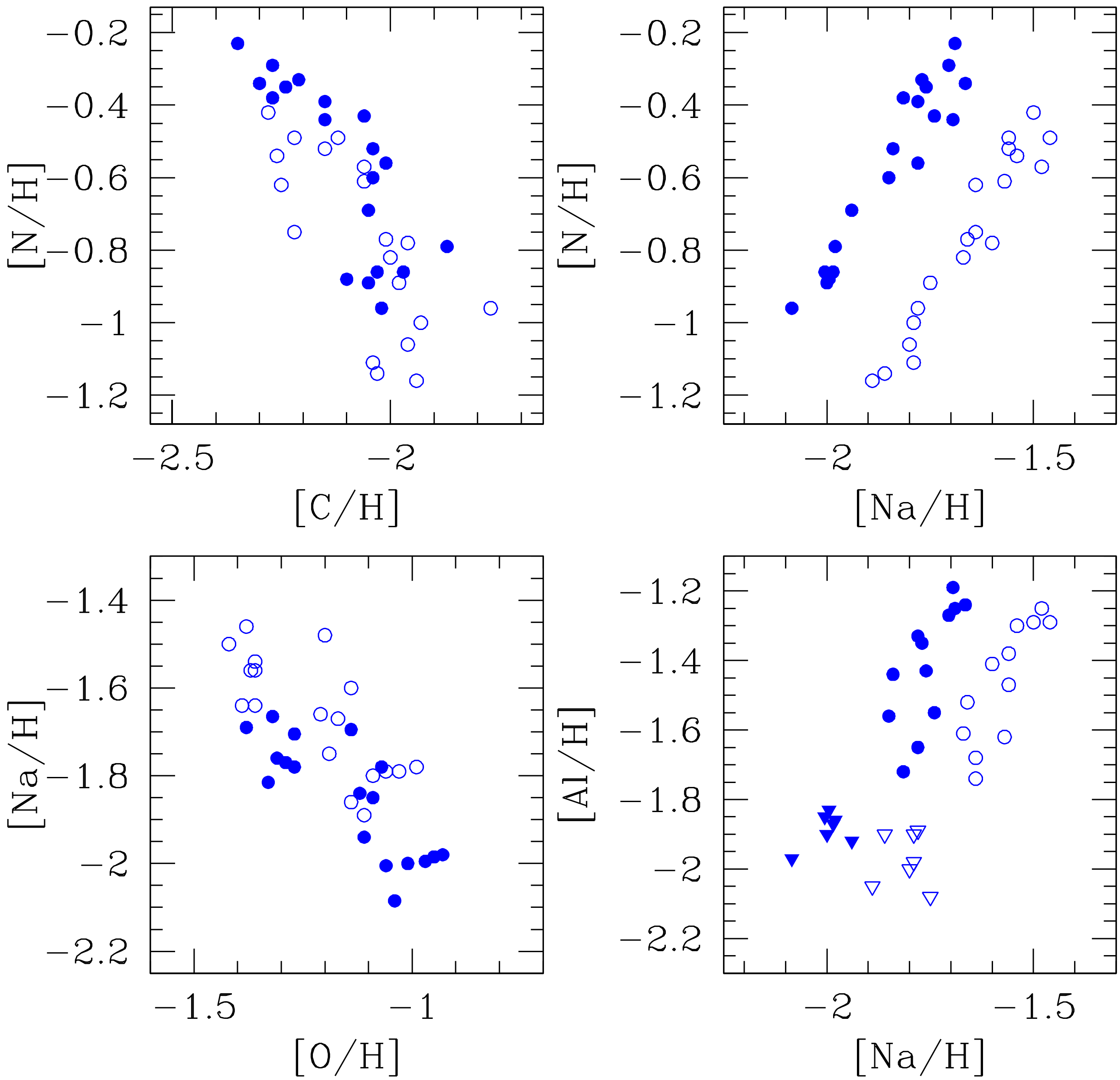

Figure 3. Light element abundance ratios (normalized to hydrogen) in the AGB stars of NGC 6752 calculated with the photometric $T_{\rm eff}$ by C17 (blue filled circles) and with the spectroscopic $T_{\rm eff}$ by L16 (blue empty circles). Reversed triangles indicate upper limits for [Al/H].

the two $T_{\rm eff}$ scales leads to a systematic offset in the abundance ratios without changing the chemical patterns already detected by L16 with the spectroscopic $T_{\rm eff}$.

L16 show in their Figure 1 the comparison between the spectra of two AGB cluster stars (namely #44 and #65) with similar parameters but different depths concerning Na, O, and Al atomic lines and CN and NH molecular bands, and similar depths for the other metallic lines. In Figure 4 we show the spectral regions around the Na I doublet at 5682–88 Å (upper panel) and the forbidden O I line at 6300.3 Å (lower panel) for these two stars. C17 provide very similar photometric $T_{\rm eff}$ (with a difference of 26 K only) for these two stars. Hence, the use of their $T_{\rm eff}$ scale cannot explain the different depths of these molecular and atomic lines, which can be attributed only to an intrinsic chemical abundance difference.

Figure 5 shows the trend between [Na/H] and [O/H] for the AGB (blue circles) and the RGB (red squares) stars when the photometric $T_{\rm eff}$ is adopted. For [O/H] > −1.4 dex, an offset is found between the Na abundances of the two groups of stars, with [Na/H] in the AGB stars being lower by −0.1 dex than that measured in the RGB stars. The origin of this small offset is unclear but it cannot be attributed to systematics in the analysis, because we adopted the same line list, solar values, $T_{\rm eff}$ scales, and NLTE corrections (the latter from Lind et al. 2011) for the two stellar samples. Despite this offset, the two samples exhibit a clear Na–O anticorrelation, showing a different extent. In agreement with the results of L16, objects with the highest Na and the lowest O abundances observed among the RGB stars are missing along the AGB (see also Yong et al. 2003; Carretta et al. 2009).

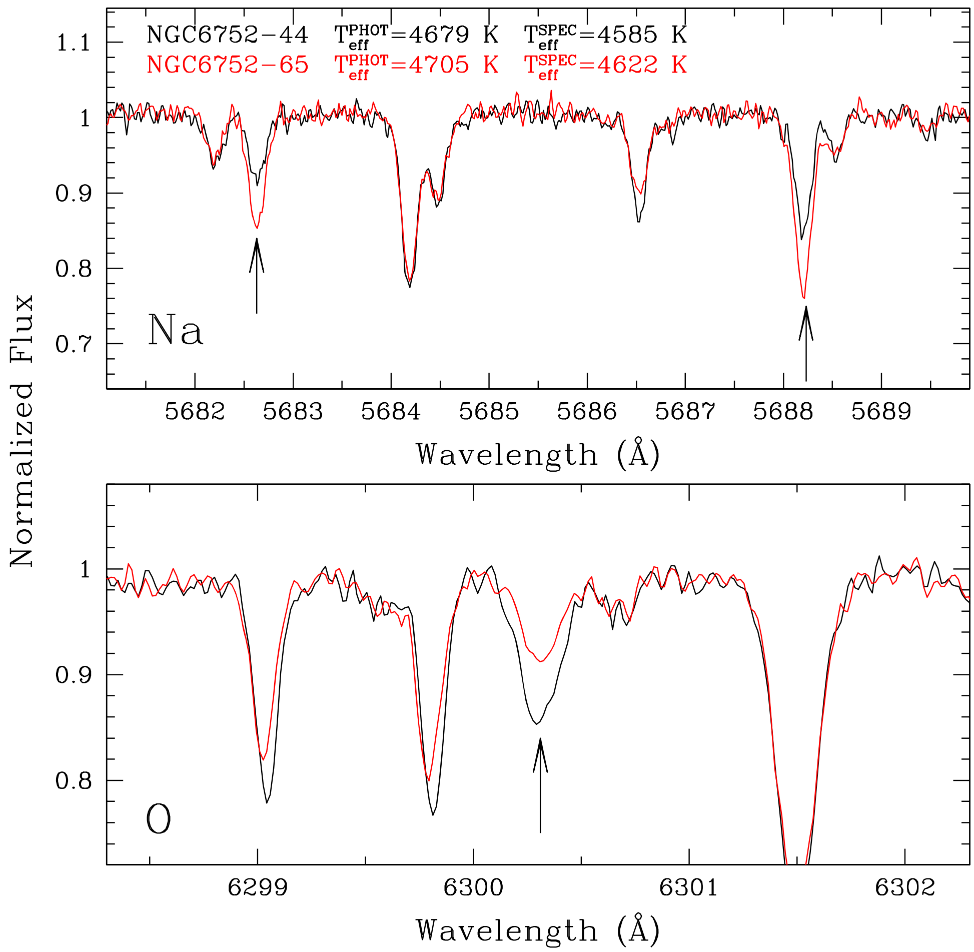

Figure 4. Comparison between the spectra of the AGB stars #44 and #65 (black and red line, respectively), in the spectral regions around the Na I doublet (upper panel) and the forbidden O I line (lower panel). Photometric and spectroscopic T_{eff} for the two targets are labeled in the upper panel.

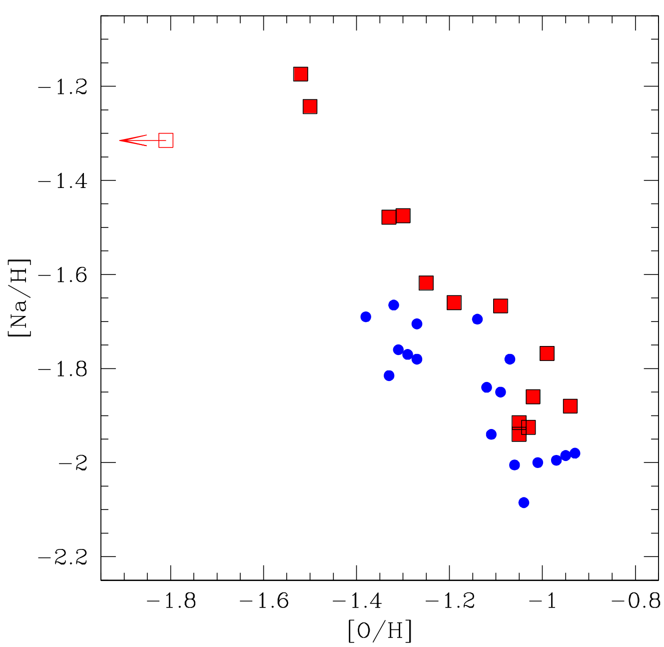

Figure 5. Behavior of [Na/H] as a function of [O/H] for the AGB and the RGB stars (blue circles and red squares, respectively) measured adopting the photometric T_{eff}. The arrow indicates an upper limit for [O/H].

Hence, also the light element abundances obtained by using the photometric T_{eff} support the conclusion by L16: the AGB stars in NGC 6752 include a mixture of 1P and 2P stars. Indeed, the existence of clear chemical patterns among the light element abundances of AGB stars is not compatible with the presence of 1P stars only. This result agrees with theoretical predictions for NGC 6752 (Cassisi et al. 2014) and with the evidence based on Strömgren photometry provided by Gruyters et al. (2017) that demonstrates the presence of three subpopulations in the RGB of the cluster but only two subpopulations in the AGB. In particular, the position of the 1P and 2P stars as identified by L16 according to their Na and O abundances correlates well with the two photometric branches observed along the AGB.

5. AGB versus RGB: Some Missing Physics?

The comparison between the spectroscopic and $(V-K)_0$-based T_{eff} in RGB and AGB stars of NGC 6752 provides an unexpected result. As discussed in Section 4, photometric and spectroscopic T_{eff} agree very well in RGB stars but they are different by ∼100 K in AGB stars. The spectra of the two stellar samples are very similar in terms of spectral coverage, spectral resolution, and signal-to-noise ratio. Also, the analysis of AGB and RGB stars is

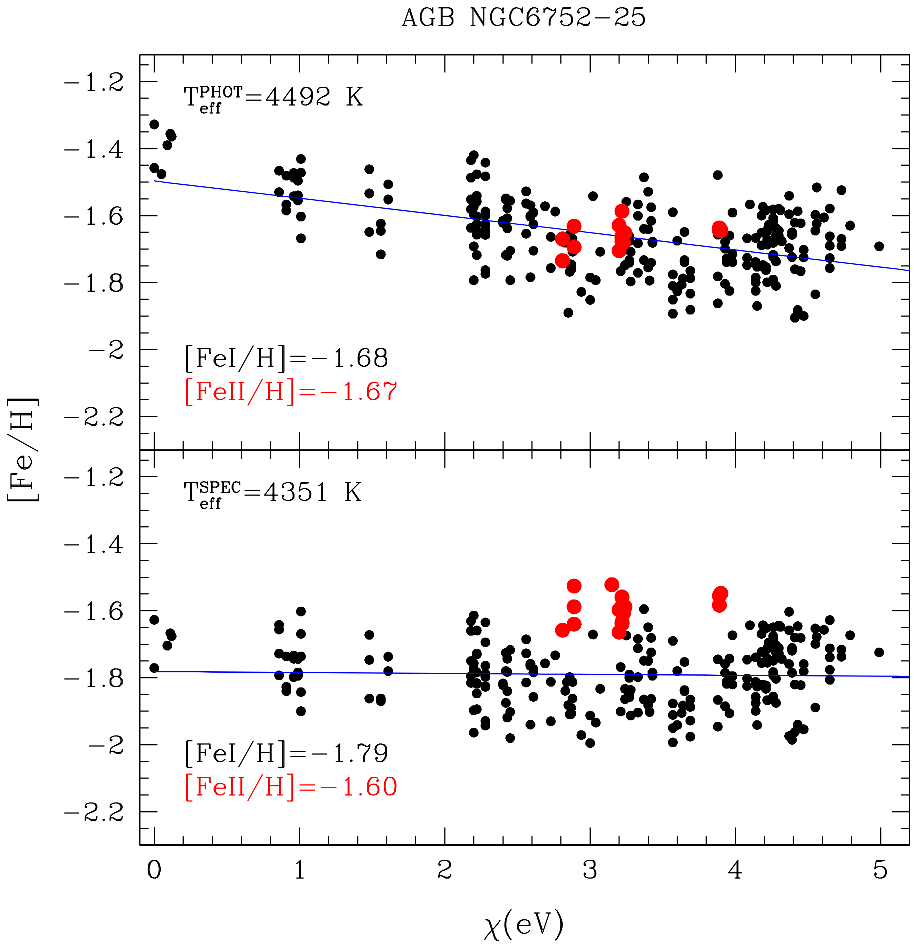

Figure 6. Behavior of the iron abundances as a function of the excitation potential, χ, for the AGB star #25, in the case of the photometric T_{eff} adopted by C17 (upper panel) and of the spectroscopic T_{eff} derived by L16 (lower panel). The black circles are for the abundances derived from neutral Fe lines and the red circles are for the single ionized Fe lines. The blue lines are the best linear fits obtained to the Fe I abundances.

based on the same line list and the same model atmospheres. Hence, this different behavior cannot be attributed to some systematics in the analysis.

Figure 6 shows the behavior of the iron abundances as a function of χ for the AGB star NGC 6752-25, for which a difference of about 150 K is found between photometric and spectroscopic T_{eff}. While a good agreement between [Fe I/H] and [Fe II/H] is derived using the photometric T_{eff}, this temperature scale introduces a significant slope between [Fe I/H] and χ. This trend is canceled out by adopting a cooler T_{eff} but this also increases the difference between the abundances from Fe I and Fe II lines, thus increasing the iron discrepancy. Note that the spectra used by C17 have a small number of Fe I lines (and without lines with $\chi < 2$ eV) and they are not suitable to highlight that photometric T_{eff} do not satisfy the excitation equilibrium.

The only way to satisfy the excitation equilibrium adopting the photometric T_{eff} is to increase v_t by 0.3–0.5 km s^{-1} (changes in log g do not impact the slope between [Fe I/H] and χ). However, this choice has two disadvantages: it introduces a significant, negative slope between [Fe I/H] and the reduced equivalent width (i.e., the stronger lines provide systematically lower abundances), pointing out that these v_t are wrong, and the derived average iron abundances (both from Fe I and Fe II lines) are ~0.1 dex lower than those obtained for RGB stars. In other words, there is no way for the AGB stars to satisfy all the spectroscopic constraints adopting photometric T_{eff} (at variance with the RGB stars).

As an additional check, we analyzed the AGB stars with the *hybrid method* (see Section 3) excluding Fe I lines with $\chi < 2$ eV that are the most sensitive to T_{eff} and to 3D and NLTE effects (see, e.g., Collet et al. 2007; Mashonkina et al. 2013; Amarsi et al. 2016). Also with this selection, a significant slope between [Fe I/H] and χ is found, and it can be flattened only decreasing T_{eff} with respect to the photometric values. The average difference between the spectroscopic T_{eff} derived including all the lines and those obtained by using only the high-χ ones is of −40 K ($\sigma = 37$ K). In addition, a discrepancy between the two iron abundances in AGB stars remains, with [Fe I/H] = -1.79 ± 0.01 dex ($\sigma = 0.07$ dex) and [Fe II/H] = -1.62 ± 0.01 dex ($\sigma = 0.03$ dex), while no significant difference is found for the RGB stars when the low-χ lines are excluded ([Fe I/H] = -1.61 ± 0.01 dex, $\sigma = 0.02$ dex, [Fe II/H] = -1.58 ± 0.01 dex, $\sigma = 0.03$ dex).

The difference between the two T_{eff} scales has already been discussed by C17, who suggest that it is due the tendency of the spectroscopic T_{eff} to remain close to the initial guess value (in other words, if the prior for T_{eff} is incorrect, the derived spectroscopic T_{eff} will also be incorrect). However, the GIRAFFE-FLAMES spectra analyzed by C13 and C17 have been acquired with two gratings (HR11 and HR13) that do not guarantee a robust determination of the spectroscopic T_{eff}, because of the limited spectral coverage and the low number of available lines. Using the same archival data analyzed in C13 and C17, we noted that all the unblended and usable Fe I lines available in the two gratings have excitation potentials higher than ~2 eV. The lack of low-χ Fe I lines (that are the most sensitive to T_{eff}), combined with a relatively small number of Fe I lines (less than 40, compared with more than 200 lines available in the UVES spectra) makes the spectroscopic determination of T_{eff} highly uncertain. This explains why C17 concluded that "the spectroscopically determined temperatures tend to lie close to the initial estimates." We verified what happens in the case of UVES spectra by adopting different starting values of T_{eff}. For each star, we find that the resulting spectroscopic T_{eff} converge to very similar values (with changes of less than ±20 K) regardless of the starting value.

The fact that the two T_{eff} scales agree in RGB stars but not in AGB stars is unexpected and not easy to explain. The two groups of stars have the same metallicity because they belong to the same cluster and the difference in atmospheric parameters is not large enough to justify this finding. This seems to suggest that the standard treatment of model atmospheres and line transfer is unable to properly reproduce the thermal structure of AGB stars (at variance with the RGB stars where no significant problem is found). It is hard to say which T_{eff} is correct for the AGB stars. If we assume that photometric T_{eff} are correct, we need to explain why the excitation equilibrium is not satisfied in AGB stars. On the other hand, if we rely on the spectroscopic ones, we need to explain why T_{eff} based on the $(V-K)_0$ colors (a standard and reliable temperature indicator) provide discrepant results between AGB and RGB stars. The hypothesis that 3D and/or NLTE effects are larger in AGB stars with respect to RGB stars cannot be totally ruled out and, indeed, it might also account for the small offset in [Na/H] that we found between AGB and RGB stars (see Figure 5).

6. Summary and Conclusions

The comparison between the chemical abundances in the AGB and RGB stars of NGC 6752 obtained adopting the photometric T_{eff} by C17 and the spectroscopic T_{eff} by L16 provides the following results:

1. The two T_{eff} scales agree very well for the RGB stars while for the AGB stars a systematic offset of ~100 K does exist. In particular, the photometric T_{eff} do not satisfy the excitation equilibrium for AGB stars (at variance with the RGB stars). In order to flatten the slope between [Fe I/H] and χ, the photometric T_{eff} should be lowered.
2. The adoption of the photometric T_{eff} alleviates the iron discrepancy in AGB stars but it does not totally erase the difference between [Fe I/H] and [Fe II/H] (which decreases from 0.23 to 0.12 dex), while for RGB stars the iron discrepancy is not found.
3. The use of photometric T_{eff} does not alter the correlations and anticorrelations found by L16 among the light elements (C, N, O, Na, and Al) confirming that both 1P and 2P stars are observed along the AGB of NGC 6752. This confirms the results of L16, while it is at odds with the conclusions of C13 and C17.
4. The use of high-resolution spectra (as GIRAFFE-FLAMES) with a relatively small spectral coverage (hence with a low number of Fe lines) should be avoided in the study of AGB stars because it does not allow us to properly check the occurrence of possible correlations between [Fe I/H] and χ.
5. The failure of photometric T_{eff} to satisfy the excitation equilibrium in AGB stars (but not in RGB stars) seems to suggest that current model atmospheres are not adequate to properly reproduce the complex thermal structure of these stars. In this case, neither the photometric nor the spectroscopic T_{eff} can be considered reliable. In light of these results, Fe II lines are the most robust metallicity indicators for the AGB stars.

The iron discrepancy in AGB stars remains an open problem that calls for new and deep investigations, using high-resolution, high-quality spectra for the chemical analysis and an effort to better understand the structure of the photospheres of these stars.

We thank the anonymous referee for useful comments. We thank Y. Momany for sharing with us the photometric catalog of NGC 6752. C.L. acknowledges financial support from the Swiss National Science Foundation (Ambizione grant PZ00P2_168065).

Software: GALA (Mucciarelli et al. 2013), DAOSPEC (Stetson & Pancino 2008), 4DAO (Mucciarelli 2013), SYNTHE (Sbordone et al. 2004; Kurucz 2005).

ORCID iDs

A. Mucciarelli https://orcid.org/0000-0001-9158-8580

References

Amarsi, A. M., Lind, K., Asplund, M., Barklem, P. S., & Collet, R. 2016, MNRAS, 463, 1518
Bastian, N., & Lardo, C. 2018, ARA&A, 56, 83
Bergemann, M., Lind, K., Collet, R., Magic, Z., & Asplund, M. 2012, MNRAS, 427, 27
Blackwell, D. E., & Shallis, M. J. 1977, MNRAS, 180, 177
Campbell, S. W., D'Orazi, V., Yong, D., et al. 2013, Natur, 498, 198
Campbell, S. W., MacLean, B. T., D'Orazi, V., et al. 2017, A&A, 605, 98
Carretta, E., Bragaglia, A., Gratton, R., & Lucatello, S. 2009, A&A, 505, 139
Casagrande, L., Ramirez, I., Melendez, J., Bessell, M., & Asplund, M. 2010, A&A, 512, 54
Cassisi, S., Salaris, M., Pietrinferni, A., Vink, J. S., & Monelli, M. 2014, A&A, 571, 81
Collet, R., Asplund, M., & Trampedach, R. 2007, A&A, 469, 687
Dekker, H., D'Odorico, S., Kaufer, A., Delabre, B., & Kotzlowski, H. 2000, Proc. SPIE, 4008, 534
Ferraro, F. R., Messineo, M., Fusi Pecci, F., et al. 1999, AJ, 118, 1738
Gratton, R. G., Carretta, E., & Bragaglia, A. 2012, A&ARv, 20, 50
Gratton, R. G., Carretta, E., & Castelli, F. 1996, A&A, 314, 191
Greggio, L., & Renzini, A. 1990, ApJ, 364, 35
Gruyters, P., Casagrande, L., Milone, A. P., et al. 2017, A&A, 603, 37
Harris, W. E. 1996, AJ, 112, 1487
Ivans, I. I., Kraft, R. P., Sneden, C., et al. 2001, AJ, 122, 1438
Kurucz, R. L. 2005, MSAIS, 8, 14
Laird, J. B., Rupen, M. P., Carney, B. W., & Latham, D. W. 1988, AJ, 96, 1908L
Lapenna, E., Lardo, C., Mucciarelli, A., et al. 2016, ApJ, 826L, 1
Lapenna, E., Mucciarelli, A., Ferraro, F. R., et al. 2015, ApJ, 813, 97
Lapenna, E., Mucciarelli, A., Lanzoni, B., et al. 2014, ApJ, 797, 124
Lardo, C., Salaris, M., Savino, A., et al. 2017, MNRAS, 466, 3507
Lind, K., Asplund, M., Barklem, P. S., & Belyaev, A. K. 2011, A&A, 528, 103

Lind, K., Bergemann, M., & Asplund, M. 2012, MNRAS, 427, 50
MacLean, B. T., Campbell, S. W., Amarsi, A. M., et al. 2018, MNRAS, 481, 373
MacLean, B. T., Campbell, S. W., De Silva, G. M., et al. 2016, MNRAS, 460, 69
Marino, A. F., Milone, A. P., Yong, D., et al. 2017, ApJ, 843, 66
Mashonkina, L., Ludwig, H.-G., Korn, A., Sitnova, T., & Caffau, E. 2013, MSAIS, 24, 120
Momany, Y., Piotto, G., Recio-Blanco, A., et al. 2002, ApJ, 576L, 65
Mucciarelli, A. 2013, arXiv:1311.1403
Mucciarelli, A., Lapenna, E., Massari, D., Ferraro, F. R., & Lanzoni, B. 2015a, ApJ, 801, 69
Mucciarelli, A., Lapenna, E., Massari, D., et al. 2015b, ApJ, 809, 128
Mucciarelli, A., Pancino, E., Lovisi, L., Ferraro, F. R., & Lapenna, E. 2013, ApJ, 766, 78
Norris, J., Cottrell, P. L., Freeman, K. C., & Da Costa, G. S. 1981, ApJ, 244, 205
Pasquini, L., Avila, G., Allaert, E., et al. 2000, Proc. SPIE, 4008, 129
Sbordone, L., Bonifacio, P., Castelli, F., & Kurucz, R. L. 2004, MSAIS, 5, 93
Skrutskie, M. F., Cutri, R. M., Stiening, R., et al. 2006, AJ, 131, 1163
Smith, G. H., & Norris, J. E. 1993, AJ, 105, 173
Stetson, P. B., & Pancino, E. 2008, PASP, 120, 1332
Vink, J. S., & Cassisi, S. 2002, A&A, 392, 553
Wang, Y., Primas, F., Charbonnel, C., et al. 2017, A&A, 607, 135
Yong, D., Grundahl, F., Lambert, D. L., Nissen, P. E., & Shetrone, M. D. 2003, A&A, 402, 985